Surface-Enhanced Raman Spectroscopy for biomedical diagnostics and imaging

Johannes Srajer[a,†], Andreas Schwaighofer [a,†] and Christoph Nowak [a,b,*]

[a] *Austrian Institute of Technology GmbH, AIT, Donau-City Str. 1, 1220 Vienna, Austria*
[b] *Center of Electrochemical Surface Technology, CEST, Viktor-Kaplan-Straße 2, 2700 Wiener Neustadt, Austria*

Abstract. Surface-enhanced Raman spectroscopy (SERS) is an analytical technique exploiting plasmonic effects that enhance sensitivity significantly, compared to conventional Raman spectroscopy. Progress in nanotechnology led to new fabrication methods for nanostructures and nanoparticles over the last decade. Besides increased comprehension of mechanisms that cause the signal enhancement, computational methods have been developed to tailor analyte-specific nanostructures efficiently. The ability to control the size, shape, and material of surfaces has facilitated the widespread application of SERS in biomedical analytics and clinical diagnostics. In this review, a brief excerpt of such SERS applications is shown, with special focus on cancer diagnostics, glucose detection and *in vivo* imaging applications. Simulation techniques are discussed to show that electro-dynamic theory can be used to predict the characteristics of nanostructure arrangements. Different fabrication methods, such as nanoparticle synthesis, their immobilization and lithographic methods are reviewed in brief.

Keywords. Surface-enhanced Raman spectroscopy, SERS, glucose, cancer, in vivo, nanostructure fabrication, lithography, nanoparticles, plasmonics, Mie theory DDA, FDTD, imaging

This paper was published by Biomedical Spectroscopy and Imaging, DOI: 10.3233/BSI-120034.

1. Introduction

During the last decade, the evolving field of life sciences has led to a growing need of sensitive optical techniques for biosensing, biomedical diagnostics, pathogen detection, gene mapping and DNA sequencing [1-2]. Nanostructures are powerful analytical tools based on two of their inherent key features. Firstly, the local field enhancement around the nanostructures allows detection of very few molecules, enabling low limits of detection down to single molecules. Secondly, substrates decorated with nanoparticles (NPs) provide much larger surface areas than their macroscopic dimensions indicate and therefore provide an improved sensitivity. Surface-enhanced Raman spectroscopy (SERS) became popular within the scientific community, because of its non-invasive nature and varied applications for *in vivo* assemblies. For example, it allows

[†] These authors contributed equally to the work.

simultaneous detection of multiple analytes (multiplexing) and reduces the need for labeling markers [2-3].
In general, Raman spectroscopy is an analytical method to detect chemical and biological samples. It is based on inelastic scattering of laser light on atoms or molecules [4]. Compared to other analytical methods, Raman spectroscopy suffers from an inherently small cross-section (*e.g.* 10^{-30} cm^2 per molecule) thus reducing the possibility of detecting analytes in low concentrations [2]. During the last three decades, much effort has been put into finding ways to overcome this deficit. In the early 1970s, Fleischmann *et al.* observed enhanced signal intensity when analyzing pyridine adsorbed onto electrochemically roughened silver electrodes. After this enhancement was confirmed by Jeanmaire *et al.* and Albrecht *et al.*, it became evident that NPs also enhance Raman signals [5-7]. This enhancement is caused by excitation of localized surface plasmon resonances (LSPR), which are electromagnetic waves that enhance the electromagnetic field near to the metallic nanostructures [8-10]. In the 1980s, electro-dynamical models have been developed to predict optical properties of substrates which can be used for SERS. Further, the first analytical applications of SERS, like the detection of cyanopyridines, have been developed [11-13]. Major achievements in analytics were the single molecule detection and DNA based SERS probes for medical diagnosis in the mid-1990s [14-16]. The growing popularity of SERS applications in biomedical research is shown by a hundredfold increase of yearly publications from 1991 to 2011 (searching for "SERS in the literature meta database "Pubmed").
This review will address SERS applications like glucose sensors, cancer detection and *in vivo* applications used for biological imaging and medical diagnostics. Fabrication methods from NP synthesis and their immobilization on surfaces, to lithographic methods and combinations thereof, will also be discussed. Finally, the most commonly used simulation techniques, including a very short introduction to the electromagnetic theory on LSPR, are reviewed in brief. In order to cover a wide spectrum from the fabrication of substrates to the latest biomedical applications, the authors can only provide a very concise outline to each single topic.

2. SERS Applications

Today's applications of SERS techniques are manifold. For applications in the general field of analytical chemistry, we refer the reader to recent reviews [17-18]. In bioanalytical applications, SERS substrates are used with and without the need for labeling in genetics and proteomics [19-20]. Beside the above applications, recognition of biomarkers released from bacterial spores [21-24], DNA or RNA analysis [25-27], medical diagnostics [2,28-31] and the detection of biological warfare agents [29,32-35] can be found.
The SERS effect is not substrate-bound, but can also be used in form of soluble silver or gold NPs of various sizes, for example in analytical chemistry [36-37]. In DNA biosensors, NPs allow label-free detection [38-40]. In biochemical analysis, NPs are used as labels for biomolecules functionalized with reporter molecules (*e.g.* dyes) [41-45], or with antibodies enabling the specific linking to binding sites [46-48]. Modification of the SERS labels with protective layers such as hydrophilic molecules [46], silica shells [41-42] or layer-by-layer deposited polyelectrolyte [49] has achieved robust sensing devices. An upcoming field for applications of NPs is the *in vivo* diagnosis of cancer [50-54] and related imaging techniques [55-57].

The following sections focus on SERS applications for glucose sensing, cancer diagnostics and *in vivo* applications for imaging in more detail.

2.1. Towards in vivo glucose detection with SERS sensors

An intriguing application of SERS in biomedical sensing is the real-time and quantitative detection of drugs and hormones. Especially *in vivo* diagnostics of glucose experienced considerable progress during the last few years. A significant healthcare challenge of the 21st century is the growing incidence of diabetes mellitus, a metabolic disease characterized by the patient's high blood sugar level. Two types of diabetes are known, either the body does not produce its own insulin (Type I), or cells do not respond to the insulin that is produced (Type II). Successful treatment makes it necessary to quantitatively monitor the blood sugar level over time to determine the right dosage of medication. The currently most prevalent but invasive "finger-stick" method is based on the electrochemical detection of hydrogen peroxide, the redox species produced by enzymatic reduction of glucose by glucose oxidase [58-59]. Other indirect techniques relying on protein-glucose interaction [60-61] have similar limitations *i.e.* finite protein stability [62] and liability to false positives by interfering analytes [58-59,63]. For direct detection of glucose, a number of laboratory techniques are established [64-65]. Unfortunately, these methods are limited for application in medical diagnostics, in particular for everyday clinical or personal use because of their size and cost.

Optical techniques for the direct glucose determination, like polarimetric [66-67], infrared [68-69] and Raman scattering methods [70-71] have been developed. The polarimetric methods lack specificity due to interferences of other chiral molecules [72]. In IR spectroscopy, the competing absorbance of water and difficulties in producing miniaturized broad-band light sources are the challenges for routine application. The initial drawbacks of Raman scattering methods, such as long acquisition times and high powers not feasible in biomedical applications have been overcome with the employment of SERS [73].

The Van Duyne group showed recently that SERS is applicable for real-time *in vivo* analysis of a complex biological matrix under varying conditions. In order to monitor glucose levels over time, an *in vivo* glucose sensor needs to be specific, reversible and stable. To accurately determine physiologically relevant glucose concentrations, a fast temporal response of the sensor is necessary. In 2003, the first *in vitro* glucose sensor based on SERS was introduced, using a Ag film over a nanospheres architecture (AgFON) [73]. Because of the low intrinsic affinity of glucose towards noble metal surfaces, a self-assembled monolayer (SAM) was used to preconcentrate glucose within the range of electromagnetic enhancement. Initially, alkanethiol monolayers were used, but the SAM composition was optimized later on as described below [74]. Since the SAM layer acts like a stationary phase in chromatography, it partitions and also departitions glucose on AgFON, thus providing reversible conditions for long term measurements [62]. By avoiding direct contact of analytes with the metal surface, the nanostructures are prevented from fouling. A quantitative real-time analysis of glucose at physiological levels has been achieved in presence of interfering analytes and bovine plasma using multivariate analysis [63]. Transferring an *in vitro* technique to the living object generally poses a challenging task and was addressed by implanting the AgFON nanostructure in the interstitial space between muscle and dermis of a Sprague-Dawley rat as a live animal model [75]. Difficulties in this approach were the surgical

placement of the implant without causing damage to the host or sensor surface as well as interfering effects on the sensor immersed in the biological milieu. Non-target molecules such as clotting factors and other blood constituents may create interfering signals and noise while blocking the analyte from accessing the sensor surface. These problems were solved by developing a mixed SAM consisting of decanethiole (DT) and mercaptohexanol (MH). Thus creating a stable, biocompatible surface that can be used as internal standard and resists non-specific binding of proteins [75-77]. The accuracy of blood glucose concentration in the interstitial fluid acquired by SERS using an optical window is comparable to that of commercial glucometers [75,78].
The latest developments of *in vivo* glucose sensors were achieved by combining the AgFON DT/MH sensor and spatially offset Raman spectroscopy (SORS). Unlike in conventional Raman spectroscopy, where the points of excitation and collection are coincident, the Raman scattered light is collected from regions offset from the laser excitation area in SORS [79]. SORS highlights the spectral features of underlying layers compared to the actual surface that gives a greater contribution in the Raman spectrum. The combination of highly sensitive SERS and the depth resolution of SORS led to the new transcutaneous glucose sensor, shown in Fig. 1 [80]. Long term stability of up to 17 days without calibration and a lower limit of detection than clinically required have been shown for this technique [81].

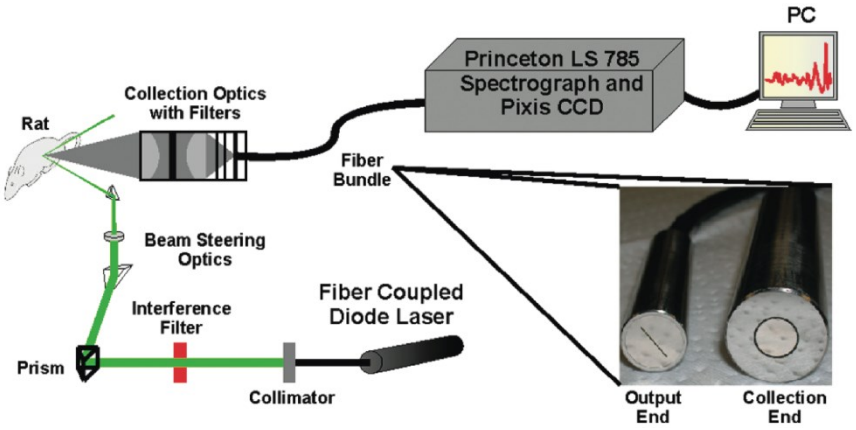

Fig. 1. Scheme of the surface-enhanced spatially offset Raman spectroscopy (SESORS) device. The inset shows the annular fiber bundle used to achieve offset collection. Reprinted with permission from [80]. Copyright 2010 American Chemical Society.

2.2. SERS-based cancer diagnostics

The use of nanostructures and nanoparticles for cancer-related diagnostics has become an extremely active field during the last few years. With cancer posing one of the most challenging medical problems, it is expected that the development of nanoparticle-based technologies improves cancer diagnosis and treatment. Methods for diagnosis of cancer using conventional Raman spectroscopy have been reported previously, but these are based on investigation of cancerous tissues after the disease has advanced [82-86]. Different from normal Raman spectroscopy that provides molecular information of the entire cell, SERS techniques allow the detection and identification of

single molecules under ambient conditions [87-88], thus enabling cancer detection at an earlier stage. The high signal intensity and sensitivity qualifies SERS for application in read out immunoassays and biomarker detection. Immunoassays have become the dominant test method for detection of tumor markers *i.e.* specific proteins that are released by the tumor into the circulation system. Conventional fluorescence detection via molecular labels is used to identify a specific antigen-antibody interaction in an immunoassay. Concentrations of tumor markers are associated with different stages of cancer. Accordingly, reliable and sensitive quantification of these molecules is significant for early clinical diagnosis of cancer [89]. Advantages of SERS are the absence of photobleaching and its narrow band width (10-100 times narrower than that of fluorescence), which leads to exceptional multiplexing capability [90-91]. Another point is the low limit of detection accompanied by the inherent surface selectivity. Yan *et al.* employed this feature by performing SERS on cell surfaces of tumor and non-tumor cell lines on Ag NP agglomerate substrates [92]. The aim is to detect changes of the lipid bilayer, glycoproteins and morphology of the cell which are all associated with carcinogenesis.

For biomarker detection, Au or Ag NPs are usually labeled with Raman reporter molecules that exhibit a strong and specific signal. The outer surface of the probes is functionalized with specific targeting molecules such as antibodies (see Fig. 2B). Yang *et al.* utilized receptor-mediated endocytosis of these extrinsic Raman labels (ERL) for distinguishing breast cancer cells from normal cells [93]. In a pioneering work, Qian *et al.* decorated the ERL with thiolated polyethylene glycol to increase the biocompatibility and achieve non-invasive cancer targeting under *in vivo* conditions in living animals [50].

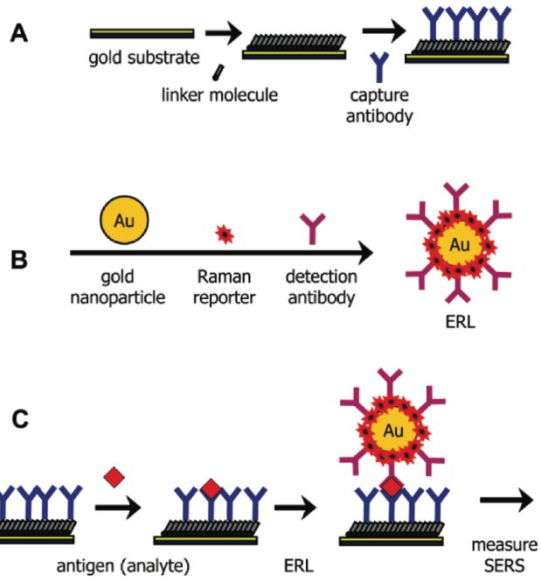

Fig. 2. General SERS-based immunoassay chip design and assay. (A) substrate functionalized with a self-assembled monolayer of linker molecules to specifically extract and concentrate antigens from solution; (B) Au NPs surface functionalized with a Raman reporter and detection antibodies (ERL), to bind to captured antigens selectively and generate intense SERS signals; (C) sandwich immunoassay with SERS readout. Reprinted with permission from [91]. Copyright 2011 American Chemical Society.

Using ERLs in combination with a capture substrate (Fig. 2A), Wang *et al.* developed a SERS based immunoassay to detect a pancreatic cancer marker molecule in serum samples (see Fig. 2C) [91]. Recently, the SERS-based immunoassay technique was used to design an optofluidic chip to analyze alpha-fetoprotein, an indicator of hepatocellular carcinoma [94]. Besides the immunoassay approach, SERS-based detection was also used on nucleic acid assays to diagnose breast cancer [90,95-96].
An entirely different approach is applied by employing the direct measurement of body fluids like blood or saliva [97-100]. Nanoparticles without any functionalization are used for signal enhancement. Olivo and *et al.* developed a Au NPs surface that allowed detection of oral cancer by evaluating spectral features of saliva samples [98]. The facile sample preparation of just mixing Au NPs with blood serum enabled Lin *et al.* to differentiate between colorectal cancer patients and healthy individuals after rigorous application of principal component analysis and linear discriminant analysis (PCA-LDA) on the SERS data [99].

2.3. In vivo applications for SERS imaging

Within the fast growing and advancing field of SERS, there has been an explosion in the number of publications reporting on SERS imaging applications, in particular employing *in vivo* imaging in living animal models. General progress in SERS imaging has been extensively reviewed recently [101-105], so the following section concerns exclusively *in vivo* imaging applications. In the field of non-invasive *in vivo* imaging, several different modalities have been used for medical diagnostics, such as nuclear imaging, magnetic resonance imaging (MRI), computer tomography, ultrasound imaging bioluminescence, and fluorescence imaging [106]. In this animate area of activity, *in vivo* imaging with SERS has gained significant interest during the last years and is about to become a predominant imaging modality [107]. Advantages over other imaging methods include low detectable amounts of targeted molecules, employment of multiplex imaging due to the narrow peak shapes and low toxicity because of the inert nature of NPs [104].
Modifications of NPs with reporter molecules (*e.g.* dyes) that exhibit a strong, unique Raman spectrum allow the detection of multiple NPs (functionalized with different Raman reporters) simultaneously. Gambhir *et al.* demonstrated multiplexing capabilities in a living mouse by intravenously administering differently tagged NPs and observing their natural accumulation in the liver [56-57]. Fig. 3 shows the transcutaneously acquired SERS spectra and images with penetration depth of up to 5 mm. Deconvolution of the SERS image (Fig. 3B), according to the unique SERS spectra of the Raman reporters (Fig. 3A) allowed the separate evaluation of the accumulation of each functionalized nanoparticle type (Fig. 3C). Further functionalization of NPs with targeting ligands (*e.g.* peptides, proteins, antibodies) is the predominant approach for tumor targeting. This technique can also be applied to *in vivo* imaging. Following the early work of Nie *et al.* [50], a growing number of *in vivo* studies involving functionalized SERS-tags were reported over the last years [108]. Recently, Maiti *et al.* demonstrated multiplexed targeted *in vivo* cancer detection, employing modified Au NPs with Raman reporters and anti-epidermal growth factor (EGFR) antibodies [54-55]. EGFR overexpression has been related to various solid tumor types such as head, neck, lung and bladder cancer. Current investigations are headed towards designing contrast agents for multimodal imaging, thus overcoming the

shortcomings of one imaging method with the advantages of the other [109-111]. MRI offers high image resolution, but suffers from poor sensitivity and low detection limit. To combine MRI with the high sensitivity yet low resolution of SERS, Yigit *et al.* reported on nanotags based on MRI-active superparamagnetic iron oxide nanoparticles. These NPs are stably complexed with SERS-active gold nanoparticles and were successfully tested *in vivo* [112].

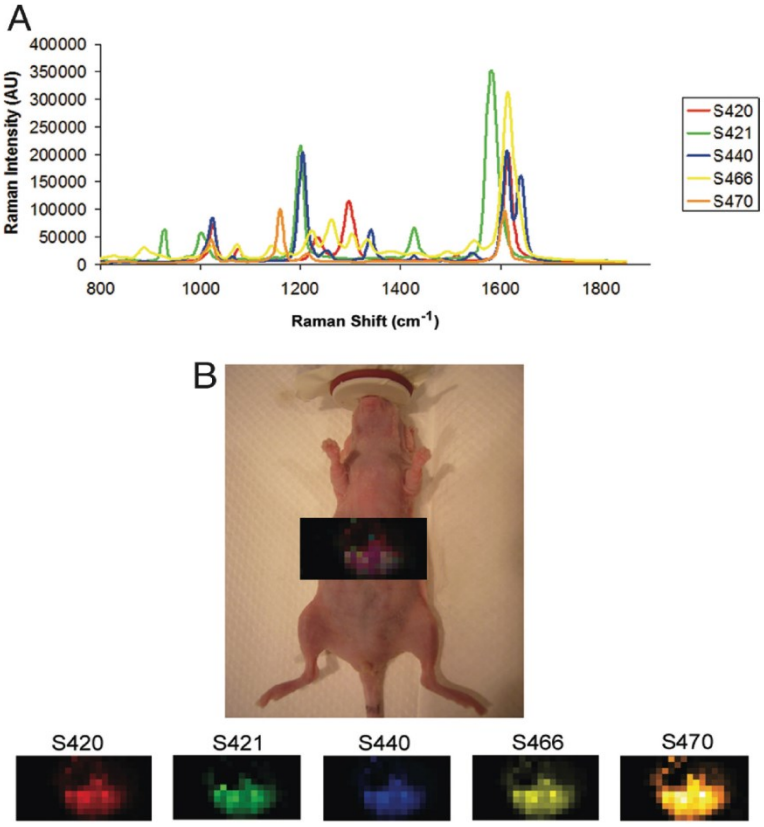

Fig. 3. Demonstration of deep-tissue multiplexed imaging of five unique SERS nanoparticle batches simultaneously. (A) Graph depicting the Raman spectra of the five individual SERS batches. (B) Raman image of liver overlaid on digital photo of mouse, showing accumulation of all five sorts of NPs accumulating in the liver. Panels below depict separate channels associated with each of the injected SERS nanoparticle batches. Individual colors have been assigned to each channel. All NPs show accumulation in the liver, while their distribution is not homogenous [57]. Reproduced with permission by the author.

3. Surface Shapes and Fabrications

Various techniques have been reported on manufacturing structures which support the excitation of LSPR and further lead to the surface-enhancement effect [113-114]. Research on nanostructures for SERS shows extensive possibilities for optimization, since the maximum field enhancement depends strongly on the shape, size and arrangement of the metallic nanostructures [115]. While average enhancement factors

range between 10^4 and 10^5, enhancement factors as high as 10^{10} have been reported [116]. It is crucial to keep in mind, that there is no single standard procedure for determining enhancement factors. A comprehensive overview on this topic is given in a review by Le Ru *et al.* [117].
Beside the aim of maximal signal intensity, other requirements are inexpensive and easy production, as well as reproducibility. A common compromise is to employ fabrication methods that have average enhancement, but provide good reproducibility. For a facile overview, we discuss the manufacturing methods for nanostructure arrangements as follows: firstly, chemical production of NPs and their immobilization onto substrates and secondly, fabricated nanostructures using lithographic methods and combinations of nanoparticles with lithographic methods.

3.1. Nanoparticles and Immobilization

The process of creating SERS substrates that employ NPs starts with solution-phase synthesis of metal nanocrystals. Here, formation of small clusters of atoms, *i.e.* nucleation, plays a major role [118-119]. During this synthesis, citric acid can be used to establish a controllable coagulation of NPs [119-121]. When the nuclei reach a critical size, they show a relatively stable crystallinity and well defined crystallographic facets, so-called seeds [122]. The shape of the resulting seeds depends on the minimal surface energy, a distinct property of the materials in use. A common crystallographic defect within these seeds is called twinning. It occurs under low temperatures and can be understood in terms of minimization of the surface energy [123]. While the twinned seeds are of almost spherical shape, several different shapes of nanocrystals can be grown. The shape depends on the growth rate along the different directions of the crystal structure, as shown in Fig. 4 [124-125].
In the next step, the metallic nanoparticles have to be deposited onto the substrate. The most commonly used method is the self-assembly of nanoparticles using bifunctional molecules, primarily reported by the Natan group [126]. Amine or thiol groups are commonly used as bifunctional anchor molecules that bind to the substrate on the one side and to the NPs on the other [127-128]. This self-assembly method also works for non-flat materials, as demonstrated using 4-aminobenzenethiol to immobilize Ag NPs onto Ag nanowires [129]. The latest developments showed that 3D structures, made out of multiple self-assembled NP layers show a SERS signal that is about two orders of magnitude higher than that of single NP layers [3,130-131]. Besides these more common methods, other modification methods have been established. For instance using silane-chemistry is used to increase sample-to-sample reproducibility [121,132]. Self-assembly due to electrostatic interaction of polymers and biomolecules such as proteins, antigens and nucleic acid systems has also been reported [133-137].

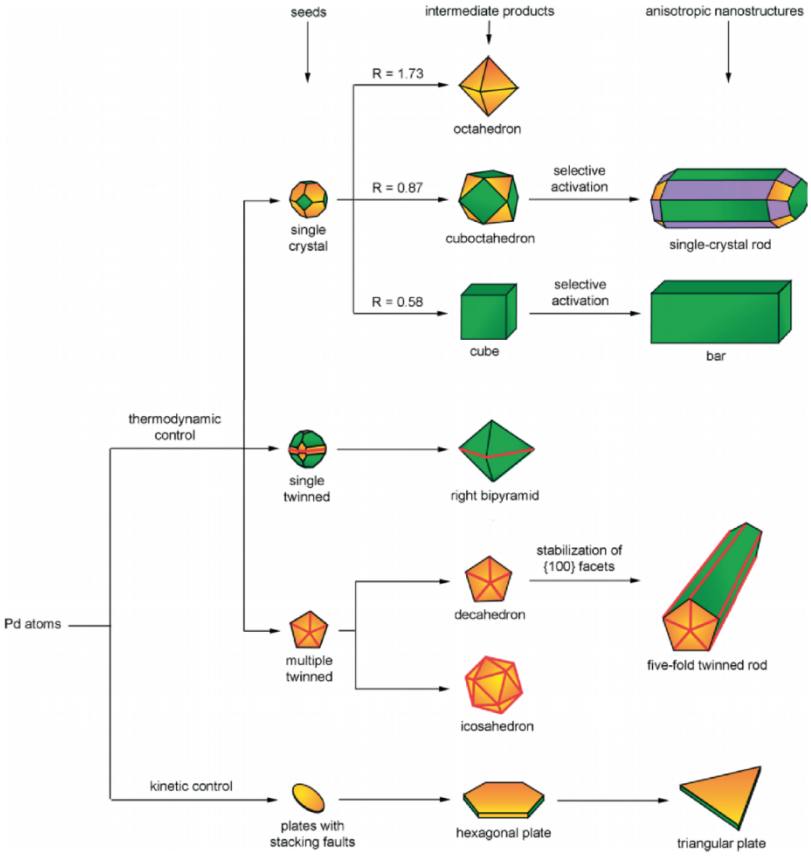

Fig. 4. Illustration of reaction pathways that lead to differently shaped NP using Pd. Once the nuclei have grown past a certain size, the seeds become single or multiple twinned, or single crystalloid, respectively. The colors green, orange, and purple represent the different crystallographic facets <100>, <111> and <110>. Twinning planes are marked in red, and R is defined as ratio between the growth rates along the <100> and <111> direction. From [122], Copyright © 2007 by John Wiley & Sons, Inc. Reprinted by permission of John Wiley & Sons, Inc.

3.2. Nanolithographic Methods and Combinations

The ongoing miniaturization in semiconductor technologies made it possible to develop lithographic methods that provide resolutions far below the 100 nm mark. Nowadays nanolithographic methods are manifold and span atomic force microscope nanolithography, neutral particle lithography, photo- and X-ray lithography [138-140]. By far the most common fabrication methods are photo- and electron-beam nanolithography. Both are based on chemical resists sensitive to the exposure of the incident light- or electron-beam. Positive and negative resists are available. For the positive resist, areas exposed to the beam will be soluble in the developer, so that the resist will be rinsed away in these areas during the following washing step. Negative resists work the opposite way. The most used positive resist in electron beam lithography is poly-methyl methacrylate [17]. There are two different methods of

fabricating substrates, the lift-off technique and reactive ion etching. Nanoparticle arrays are normally created using the lift-off-method, while linear and crossed gratings are typically transferred onto a substrate by reactive ion etching method (see Fig. 5) [17]. In performance evaluation of both methods for gold, the continuous film approach lead to better results than the isolated NPs substrate [141].

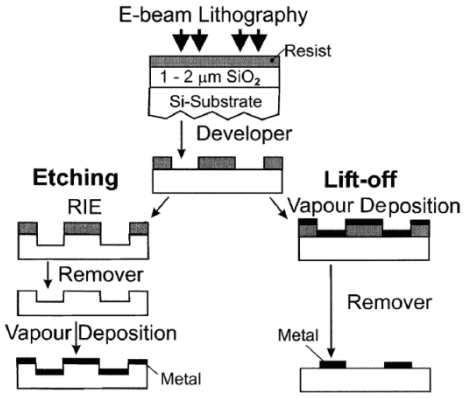

Fig. 5. Scheme of etching and lift-off fabrication strategies for SERS substrates. In the etching process, the substrate is covered with metal on the whole surface. Using lift-off, the substrate presents a series of isolated NPs, after the removal of the resist. From [141]; Copyright © 1998 Elsevier B.V. Reprinted by permission of Elsevier B.V

The most important advantage of lithography is the possibility to control NP size, shape and arrangement with great accuracy. Numerous studies on distance and shape dependency of the plasmon resonance positions, and differences between NP gratings and nanohole gratings can be found in literature [142-144]. In highly ordered arrangements of NPs, plasmonic grating resonances, also called propagating surface plasmons (PSP), can be excited in addition to LSPR. PSP generation depends on the size and environment of the NPs. Substrates combining both, PSP and LSPR have been reported to provide enhancement factors of up to $8.4\ 10^8$ [145-148]. However, even if substrates prepared by photo- or electron-beam lithography show the highest reproducibility, these methods are not suitable for mass-production because of their high cost.

A promising approach is the usage of templates that allow deposition of metals in a controllable way. A good example for that is nanosphere lithography (NSL), which was developed by Van Duyne's group [149]. In NSL, self-assembled monolayers of nanospheres are used as templates for vapor deposition of metals. After the metal is directly deposited on the nanosphere layer, the nanosphere mask is removed. This leads to a periodic structure of triangles or hexagons. The final structure depends on the number of nanosphere layers deposited onto the substrate [150-151]. Immobilization of the nanospheres is again performed using methods described in the previous section. Using NSL, Van Duyne *et al.* examined the relationship between localized plasmon excitation and the SERS enhancement factor, reaching a maximum enhancement factor of 10^8 [152]. Based on NSL, nanocrescents and crescent shaped nanoholes have been developed, which exhibit multiple localized surface plasmon resonances form the visible to the infrared region [153-155].

4. Theoretical Background

Simulation techniques are typically used to adapt nano-structured geometries for biosensing applications to develop made-to-measure devices. Several excellent reviews on the theoretical background are available [156-158]. The following section describes the theory behind the interaction of light with free electrons at a metal-dielectric interface, approximate solutions and numerical simulation methods.

Even though surface plasmon polaritons are named in a way that sounds similar to quantum quasiparticles, the classical description based on Maxwell equations is suitable to describe the electron waves resulting from interactions between electrons and photons at interfaces [157]. In a review from Gustav Mie on the optics of metallic colloidal solutions, the scattering problem of a polarized plane wave on a spherical metal-particle in a non-conductive solution has been addressed [159]. The usage of spherical coordinates helped Mie to find the first approximation to the scattering problem for NPs in solution. The resulting wave can be developed in an infinite series, similar to multipole expansion in electric fields. The accuracy of the predicted wavelengths of the plasmon resonances, when compared to scattering experiments, made "Mie scattering" to an eponym for elastic scattering at spherical particles in the size range of the wavelength of the exciting light. This theory was then extended to spheroidal particles, taking into account oblate and prolate particles by Gans [160].

Since modern computing techniques facilitate the simulation of light scattered on objects of any shape, we will only discuss the simple example of a plane wave on the flat interface between a metal and a dielectric material, as shown in Fig. 6. Surface plasmons propagating along this interface can be described as a transverse magnetic wave, which leads to the following equations [161]. For the two sides of the interface, the magnetic field $\vec{H}$ is given by

$$\vec{H} = \hat{y}\ A_d\ exp(i\kappa\hat{x} + \alpha_d z) \qquad z < 0 \tag{1}$$

$$\vec{H} = \hat{y}\ A_m\ exp(i\kappa\hat{x} - \alpha_m z) \qquad z > 0 \tag{2}$$

with the wavevector $\kappa\hat{x}$ and its lateral wavenumber κ, the transverse wavenumbers α_d and α_m and the coefficients A_d and A_m, which have to be determined. The condition for real transverse wavenumbers can be written as

$$\alpha_d^2 = \kappa^2 - \left(\frac{2\pi n_d}{\lambda}\right)^2, \qquad \alpha_m^2 = \kappa^2 - \left(\frac{2\pi n_m}{\lambda}\right)^2 \tag{3}$$

using the free space wavelength λ and the complex refractive indices n_d and n_m of the dielectric material and the metal, respectivley. In order to satisfy the boundary conditions for the electric and magnetic fields at the interface (z=0), the Maxwell equations lead to the dispersion relation (*i.e.* the energy-momentum relation)

$$\alpha_m n_d^2 + \alpha_d n_m^2 = 0 \tag{4}$$

which is typically written in the form of

$$\kappa = \frac{2\pi}{\lambda}\sqrt{\frac{\varepsilon_d \varepsilon_m}{\varepsilon_m + \varepsilon_d}}. \quad (5)$$

The latter equation is assuming materials where the relation between the complex refractive index n and the relative permittivity ϵ is given by $n = \sqrt{\epsilon}$, assuming a relative permeability $\mu = 1$, which is a common expectation for metals at optical frequencies [162]. A few conclusions can be drawn from this simple example. One condition for a plasmon wave to exist is that the real parts of the permittivities of the metal and the dielectric need to have opposite signs. Since the permittivity functions are usually complex, the wavevector is also complex, leading to a finite propagation length of the wave. For long range propagation, for which the complex values of κ are diminishing, the condition $\varepsilon_d < -\varepsilon_m$ must hold.
Current methods for calculating the electromagnetic properties of NPs make use of different numerical techniques in order to simulate the influence of adsorbed molecules on metal films, different shapes of nanoparticles and coupling effects of regular gratings. In the following sections, the three most common simulation techniques are discussed in brief.

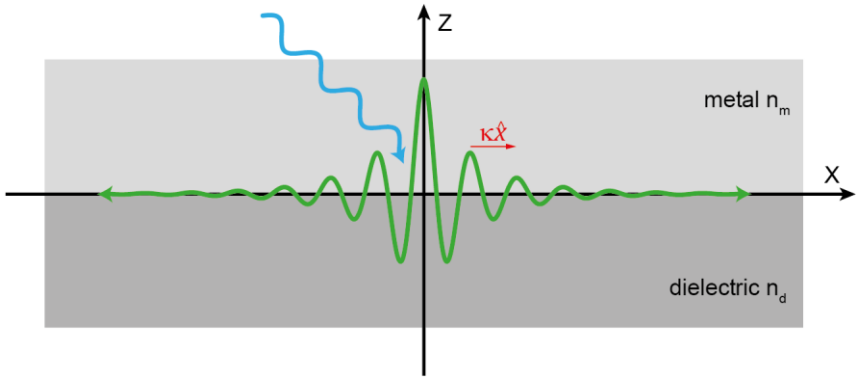

Fig. 6. Scheme of a plasmonic resonance at a metal-dielectric interface. Through an external stimulation (blue), a standing electromagnetic wave (green) can be generated, called surface plasmon resonance. The propagation length is predefined by the complex wavenumber κ. For long range propagation, the complex value of κ diminishes.

4.1. Finite Difference Time Domain (FDTD)

In 1966, Kane Yee published a method, where he replaced Maxwell equations with a set of finite difference equations [163]. In principle, the finite difference time domain method (FDTD) is based on discretization of geometries into calculation grids, in which the three components of the electric and magnetic field are stored at different positions of a single voxel (*i.e.* volumetric pixel element). Even though Yee already proposed a stability criterion, a general stability condition was introduced later by Taflove *et al.* [164]. Based on this criterion, the first validated simulation of a electromagnetic wave penetrating a metal cavity was performed [165]. The acronym FDTD reflects that the temporal evolution of the fields is calculated in this method, while the frequency domain spectra of nanoparticles have to be calculated through

Fourier transformations. FDTD advanced rapidly during the last few decades. A major milestone was the development of the so-called perfectly matched layers, which mimic an open boundary condition where electromagnetic waves are not or only barely reflected [166-167]. This effective boundary technique has been improved later by uniaxial perfectly matched layers and convolutional perfectly matched layers [168-169]. The latest development in FDTD is an unconditionally, numerically stable algorithm, which was introduced by DeRaedt and further improved by Ahmed *et al.* [170-171].
Correlations between measured and simulated spectra from reflectance, transmission, fluorescence and SPR-measurements, have proven the ability of this method to properly describe reality [145-148].

4.2. Discrete Dipole Approximation (DDA)

Another popular method for computing the optical spectrum from near field distributions of NPs is the discrete dipole approximation (DDA). Hereby, arbitrary geometries are mapped on a cubic array of voxels representing electric dipoles, each with its own polarizability function. Even if methods using individual polarizabilities to describe compositions can be traced back to Lorentz, the first de-facto DDA simulation was performed by Purcell and Pennypacker [172]. They validated their model of a spherical colloid, consisting of 136 polarizable elements, using Mie theory. Since then, several attempts to improve accuracy, numerical stability, data analysis and material assumptions have been undertaken. We kindly refer the interested reader to the review of Yurkin and Hoekstra [173].

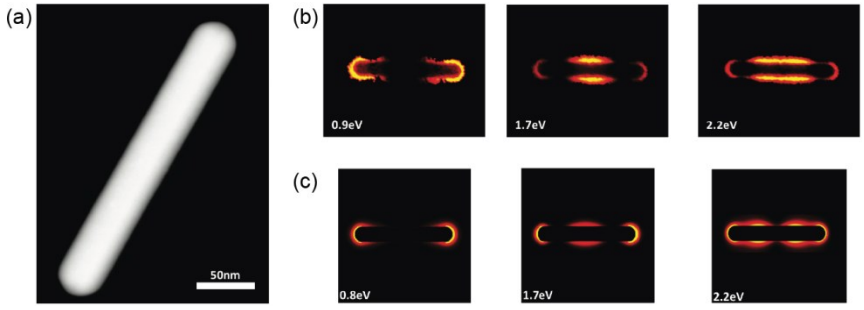

Fig. 7. Comparison between measured and simulated field strength pattern. (a) shows the geometry of the Ag nanorods, (b) illustrates the intensity image form electron energy loss spectroscopy at three different energies and (c) shows the simulated field strength of the electric field using a DDA method. Adapted with permission from [177], Copyright 2011 American Chemical Society.

For a long time, field strength patterns were exclusively accessible through simulations. Recently, the correlation between the intensity in electron energy loss spectroscopy and the electric field density, which is equivalent to the photonic density of states, showed that the simulated and real field patterns are in good agreement. As an example, Fig. 7 shows how field pattern calculated using the DDA method behave compared to electron energy loss measurements.
The most commonly used DDA code is DDSCAT, written in FORTRAN 90, which includes functions of various target geometries and periodic structures [174]. Recently, C based codes as well as Matlab based codes have been published [173,175-176].

4.3. Finite Elements Method (FEM)

A method particularly interesting for complex geometries is the finite elements method (FEM). It was first outlined by Courant [178]. A result is obtained by using the variational principle to find solutions, where every element of the mesh satisfies Gauss' law and the appropriate boundary conditions on the surface of the element [158]. A variety of mesh generation software to divide the domain into a fine grid of elements, on which the partial differential equations are solved, is available online [179]. Since FEM is also very popular for solving fluid mechanics and structural mechanics, there are many software tools for solving electro-dynamic problems as well. A review on FEM applied to electromagnetic problems was published by Coccioli *et al.* [180].
A comparison between field patterns calculated by FDTD and FEM is shown in Fig. 8. The FEM results show some small artifacts, but they agree well with the FDTD results. FDTD is more accurate, but it consumes much more computation power. In the shown example the FDTD simulation took 2058 CPU hours (á 2.8 GHz), while the FEM simulation only took four CPU hours (á 3.4 GHz) [158].

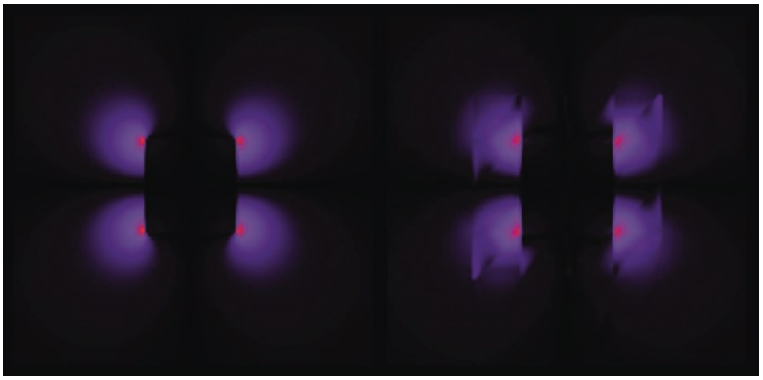

Fig. 8. Field patterns of scattered light of a cubic nanoparticle with 50 nm edge length. The left side shows the FDTD simulations and the right side the FEM simulation, respectively. Adapted with permission from [158], Copyright 2008 American Chemical Society.

Several software packages, from open-source and freeware to proprietary codes, are available. Most open-source codes are command line based, using C++ or FORTRAN libraries, while most of the commercial software packages have a graphical user interface. Due to the wide variety, an application-oriented analysis of which software satisfies the user's requirements is advisable before deciding on any simulation software. All discussed simulation methods can be used to predict the wavelengths of LSPR excitations and therefore fasten the development of new SERS applications.

5. Conclusions

In applications involving the diagnosis of cancerous lesions, the current standard is surgical resection and analysis by histopathology. Since this procedure is invasive, expensive and time-consuming, the availability of rapid, non-invasive analytical techniques is very desirable. SERS applications have shown their great potential to

become the future standard. This is not only true for cancer diagnostics but also for glucose detection. The growing number of applications in DNA sequencing using multiplexed SERS sensors, as well as progress in *in vivo* glucose detection, show that SERS has finally matured to levels of reproducibility and dependability that are needed for routine applications.

These advances also result from the rapid development of new fabrication techniques during the last decade. Thanks to lithography, the possibilities in creating new geometries are manifold. The fast evolving field of template based lithography opens the door for high-throughput analysis and minimizes expenses. The development time of new SERS applications can be further reduced by accompanying experiments with numerical simulations. Various commercial, as well as non-commercial modeling techniques are available. Knowledge of the near field behavior of a substrate is crucial for tailoring new devices.

The number of publication on SERS exploded in the past years; therefore this review only covers a fraction of those publications. Even with the high research activity on SERS, a unanimous definition of a general enhancement factor has not yet been found. In order to rate and compare different SERS techniques, a uniform definition for the enhancement factor would be highly desirable.

Acknowledgements

The authors acknowledge the contribution of B. Siebenhofer and K. Mahajan. Partial support for this work was provided by ZIT, Centre of Innovation and Technology of Vienna.

References

[1] T. Vo-Dinh, H.N. Wang, J. Scaffidi, Plasmonic nanoprobes for SERS biosensing and bioimaging, *J. Biophotonics* **3** (2010), 89-102.

[2] T. Vo-Dinh, F. Yan, M.B. Wabuyele, Surface-enhanced Raman scattering for medical diagnostics and biological imaging, *J. Raman Spectrosc.* **36** (2005), 640-647.

[3] M. Fan, A.G. Brolo, Self-Assembled Au Nanoparticles as Substrates for Surface-Enhanced Vibrational Spectroscopy: Optimization and Electrochemical Stability, *Chemphyschem* **9** (2008), 1899-1907.

[4] C.V.a.K. Raman, K.S., A New Type of Secondary Radiation, *Nature* **121** (1928), 501-502.

[5] M.G. Albrecht, J.A. Creighton, Anomalously intense Raman spectra of pyridine at a silver electrode, *J. Am. Chem. Soc.* **99** (1977), 5215-5217.

[6] M. Fleischmann, P.J. Hendra, A.J. McQuillan, Raman spectra of pyridine adsorbed at a silver electrode, *Chem. Phys. Lett.* **26** (1974), 163-166.

[7] D.L. Jeanmaire, R.P. Van Duyne, Surface raman spectroelectrochemistry: Part I. Heterocyclic, aromatic, and aliphatic amines adsorbed on the anodized silver electrode, *J. Electroanal. Chem. Interfacial Electrochem.* **84** (1977), 1-20.

[8] B. Pettinger, U. Wenning, H. Wetzel, Surface plasmon enhanced Raman scattering frequency and angular resonance of Raman scattered light from pyridine on Au, Ag and Cu electrodes, *Surf. Sci.* **101** (1980), 409-416.

[9] R.M. Hexter, M.G. Albrecht, Metal surface Raman spectroscopy: Theory, *Spectrochim. Acta, Part A* **35** (1979), 233-251.

[10] M. Moskovits, Surface roughness and the enhanced intensity of Raman scattering by molecules adsorbed on metals, *J. Chem. Phys.* **69** (1978), 4159-4161.

[11] J.C. Rubim, Surface-enhanced Raman scattering (SERS) on silver electrodes as a technical tool in the study of the electrochemical reduction of cyanopyridines and in quantitative analysis, *J. Electroanal. Chem. Interfacial Electrochem.* **220** (1987), 339-350.

[12] F. Ni, H. Feng, L. Gorton, T.M. Cotton, Electrochemical and Sers Studies of Chemically Modified Electrodes - Nile Blue-a, a Mediator for Nadh Oxidation, *Langmuir* **6** (1990), 66-73.

[13] R. Sheng, F. Ni, T.M. Cotton, Determination of purine bases by reversed-phase high-performance liquid chromatography using real-time surface-enhanced Raman spectroscopy, *Anal. Chem.* **63** (1991), 437-442.

[14] T. Vo-Dinh, K. Houck, D.L. Stokes, Surface-Enhanced Raman Gene Probes, *Anal. Chem.* **66** (1994), 3379-3383.

[15] K. Kneipp, Y. Wang, H. Kneipp, L.T. Perelman, I. Itzkan, R.R. Dasari, M.S. Feld, Single Molecule Detection Using Surface-Enhanced Raman Scattering (SERS), *Phys. Rev. Lett.* **78** (1997), 1667-1670.

[16] S. Nie, S.R. Emory, Probing Single Molecules and Single Nanoparticles by Surface-Enhanced Raman Scattering, *Science* **275** (1997), 1102-1106.

[17] M.K. Fan, G.F.S. Andrade, A.G. Brolo, A review on the fabrication of substrates for surface enhanced Raman spectroscopy and their applications in analytical chemistry, *Anal. Chim. Acta.* **693** (2011), 7-25.

[18] A. Kudelski, Analytical applications of Raman spectroscopy, *Talanta* **76** (2008), 1-8.

[19] H.T. Beier, C.B. Cowan, I.H. Chou, J. Pallikal, J.E. Henry, M.E. Benford, J.B. Jackson, T.A. Good, G.L. Cote, Application of surface-enhanced Raman spectroscopy for detection of beta amyloid using nanoshells, *Plasmonics* **2** (2007), 55-64.

[20] J.W. Chen, X.P. Liu, K.J. Feng, Y. Liang, J.H. Jiang, G.L. Shen, R.Q. Yu, Detection of adenosine using surface-enhanced Raman scattering based on structure-switching signaling aptamer, *Biosens. Bioelectron.* **24** (2008), 66-71.

[21] H.W. Cheng, S.Y. Huan, H.L. Wu, G.L. Shen, R.Q. Yu, Surface-Enhanced Raman Spectroscopic Detection of a Bacteria Biomarker Using Gold Nanoparticle Immobilized Substrates, *Anal. Chem.* **81** (2009), 9902-9912.

[22] H.W. Cheng, W.Q. Luo, G.L. Wen, S.Y. Huan, G.L. Shen, R.Q. Yu, Surface-enhanced Raman scattering based detection of bacterial biomarker and potential surface reaction species, *Analyst* **135** (2010), 2993-3001.

[23] H.W. Cheng, Y.Y. Chen, X.X. Lin, S.Y. Huan, H.L. Wu, G.L. Shen, R.Q. Yu, Surface-enhanced Raman spectroscopic detection of Bacillus subtilis spores using gold nanoparticle based substrates, *Anal. Chim. Acta.* **707** (2011), 155-163.

[24] H.W. Cheng, S.Y. Huan, R.Q. Yu, Nanoparticle-based substrates for surface-enhanced Raman scattering detection of bacterial spores, *Analyst* **137** (2012), 3601-3608.

[25] A. Barhoumi, D. Zhang, F. Tam, N.J. Halas, Surface-enhanced Raman spectroscopy of DNA, *J. Am. Chem. Soc.* **130** (2008), 5523-5529.

[26] T. Vo-Dinh, Nanobiosensing using plasmonic nanoprobes, *IEEE J. Sel. Top. Quantum Electron.* **14** (2008), 198-205.

[27] Y.H. Sun, R.M. Kong, D.Q. Lu, X.B. Zhang, H.M. Meng, W.H. Tan, G.L. Shen, R.Q. Yu, A nanoscale DNA-Au dendrimer as a signal amplifier for the universal design of functional DNA-based SERS biosensors, *Chem. Commun.* **47** (2011), 3840-3842.

[28] R.M. Jarvis, R. Goodacre, Characterisation and identification of bacteria using SERS, *Chem. Soc. Rev.* **37** (2008), 931-936.

[29] O.M. Primera-Pedrozo, J.I. Jerez-Rozo, E. De la Cruz-Montoya, T. Luna-Pineda, L.C. Pacheco-Londono, S.P. Hernandez-Rivera, Nanotechnology-based detection of explosives and biological agents simulants, *Ieee Sens. J.* **8** (2008), 963-973.

[30] J. Hu, P.C. Zheng, J.H. Jiang, G.L. Shen, R.Q. Yu, G.K. Liu, Electrostatic Interaction Based Approach to Thrombin Detection by Surface-Enhanced Raman Spectroscopy, *Anal. Chem.* **81** (2009), 87-93.

[31] J. Hu, P.C. Zheng, J.H. Jiang, G.L. Shen, R.Q. Yu, G.K. Liu, Sub-attomolar HIV-1 DNA detection using surface-enhanced Raman spectroscopy, *Analyst* **135** (2010), 1084-1089.

[32] W.F. Pearman, A.W. Fountain, Classification of chemical and biological warfare agent simulants by surface-enhanced Raman spectroscopy and multivariate statistical techniques, *Appl. Spectrosc.* **60** (2006), 356-365.

[33] F. Yan, T. Vo-Dinh, Surface-enhanced Raman scattering detection of chemical and biological agents using a portable Raman integrated tunable sensor, *Sens. Actuators, B* **121** (2007), 61-66.

[34] J.K. Daniels, T.P. Caldwell, K.A. Christensen, G. Chumanov, Monitoring the kinetics of Bacillus subtilis endospore germination via surface-enhanced Raman scattering spectroscopy, *Anal. Chem.* **78** (2006), 1724-1729.

[35] J.P. Scaffidi, M.K. Gregas, B. Lauly, J.C. Carter, S.M. Angel, T. Vo-Dinh, Trace Molecular Detection via Surface-Enhanced Raman Scattering and Surface-Enhanced Resonance Raman Scattering at a Distance of 15 Meters, *Appl. Spectrosc.* **64** (2010), 485-492.

[36] F.P. Zamborini, L.L. Bao, R. Dasari, Nanoparticles in Measurement Science, *Anal. Chem.* **84** (2012), 541-576.

[37] K. Saha, S.S. Agasti, C. Kim, X.N. Li, V.M. Rotello, Gold Nanoparticles in Chemical and Biological Sensing, *Chem. Rev.* **112** (2012), 2739-2779.

[38] H.I. Peng, B.L. Miller, Recent advancements in optical DNA biosensors: Exploiting the plasmonic effects of metal nanoparticles, *Analyst* **136** (2011), 436-447.

[39] J.N. Anker, W.P. Hall, O. Lyandres, N.C. Shah, J. Zhao, R.P. Van Duyne, Biosensing with plasmonic nanosensors, *Nat. Mater.* **7** (2008), 442-453.

[40] T. Endo, K. Kerman, N. Nagatani, Y. Takamura, E. Tamiya, Label-free detection of peptide nucleic acid-DNA hybridization using localized surface plasmon resonance based optical biosensor, *Anal. Chem.* **77** (2005), 6976-6984.

[41] B. Kustner, M. Gellner, M. Schutz, F. Schoppler, A. Marx, P. Strobel, P. Adam, C. Schmuck, S. Schlucker, SERS Labels for Red Laser Excitation: Silica-Encapsulated SAMs on Tunable Gold/Silver Nanoshells, *Angew. Chem., Int. Ed.* **48** (2009), 1950-1953.

[42] L.O. Brown, S.K. Doorn, A controlled and reproducible pathway to dye-tagged, encapsulated silver nanoparticles as substrates for SERS multiplexing, *Langmuir* **24** (2008), 2277-2280.

[43] S. Boca, D. Rugina, A. Pintea, L. Barbu-Tudoran, S. Astilean, Flower-shaped gold nanoparticles: synthesis, characterization and their application as SERS-active tags inside living cells, *Nanotechnology* **22** (2011), 055702.

[44] M. Xiao, J. Nyagilo, V. Arora, P. Kulkarni, D.S. Xu, X.K. Sun, D.P. Dave, Gold nanotags for combined multi-colored Raman spectroscopy and x-ray computed tomography, *Nanotechnology* **21** (2010), 035101.

[45] C.I. Brady, N.H. Mack, L.O. Brown, S.K. Doorn, Self-Assembly Approach to Multiplexed Surface-Enhanced Raman Spectral-Encoder Beads, *Anal. Chem.* **81** (2009), 7181-7188.

[46] M. Schutz, D. Steinigeweg, M. Salehi, K. Kompe, S. Schlucker, Hydrophilically stabilized gold nanostars as SERS labels for tissue imaging of the tumor suppressor p63 by immuno-SERS microscopy, *Chem. Commun.* **47** (2011), 4216-4218.

[47] N. Guarrotxena, B. Liu, L. Fabris, G.C. Bazan, Antitags: Nanostructured Tools for Developing SERS-Based ELISA Analogs, *Adv. Mater.* **22** (2010), 4954-4958.

[48] M.Y. Sha, H.X. Xu, M.J. Natan, R. Cromer, Surface-Enhanced Raman Scattering Tags for Rapid and Homogeneous Detection of Circulating Tumor Cells in the Presence of Human Whole Blood, *J. Am. Chem. Soc.* **130** (2008), 17214-17215.

[49] K. Kim, H.S. Lee, H.D. Yu, H.K. Park, N.H. Kim, A facile route to stabilize SERS-marker molecules on mu Ag particles: Layer-by-layer deposition of polyelectrolytes, *Colloids Surf., A* **316** (2008), 1-7.

[50] X.M. Qian, X.H. Peng, D.O. Ansari, Q. Yin-Goen, G.Z. Chen, D.M. Shin, L. Yang, A.N. Young, M.D. Wang, S.M. Nie, In vivo tumor targeting and spectroscopic detection with surface-enhanced Raman nanoparticle tags, *Nat. Biotechnol.* **26** (2008), 83-90.

[51] A. Samanta, K.K. Maiti, K.S. Soh, X.J. Liao, M. Vendrell, U.S. Dinish, S.W. Yun, R. Bhuvaneswari, H. Kim, S. Rautela, J.H. Chung, M. Olivo, Y.T. Chang, Ultrasensitive Near-Infrared Raman Reporters for SERS-Based In Vivo Cancer Detection, *Angew. Chem., Int. Ed.* **50** (2011), 6089-6092.

[52] M.S. Bergholt, W. Zheng, Z.W. Huang, Characterizing variability in in vivo Raman spectroscopic properties of different anatomical sites of normal tissue in the oral cavity, *J. Raman Spectrosc.* **43** (2012), 255-262.

[53] A.M. Mohs, M.C. Mancini, S. Singhal, J.M. Provenzale, B. Leyland-Jones, M.D. Wang, S.M. Nie, Hand-held Spectroscopic Device for In Vivo and Intraoperative Tumor Detection: Contrast Enhancement, Detection Sensitivity, and Tissue Penetration, *Anal. Chem.* **82** (2010), 9058-9065.

[54] K.K. Maiti, U.S. Dinish, C.Y. Fu, J.J. Lee, K.S. Soh, S.W. Yun, R. Bhuvaneswari, M. Olivo, Y.T. Chang, Development of biocompatible SERS nanotag with increased stability by chemisorption of reporter molecule for in vivo cancer detection, *Biosens. Bioelectron.* **26** (2010), 398-403.

[55] K.K. Maiti, U.S. Dinish, A. Samanta, M. Vendrell, K.S. Soh, S.J. Park, M. Olivo, Y.T. Chang, Multiplex targeted in vivo cancer detection using sensitive near-infrared SERS nanotags, *Nano Today* **7** (2012), 85-93.

[56] S. Keren, C. Zavaleta, Z. Cheng, A. de la Zerda, O. Gheysens, S.S. Gambhir, Noninvasive molecular imaging of small living subjects using Raman spectroscopy, *Proc. Natl. Acad. Sci. U. S. A.* **105** (2008), 5844-5849.

[57] C.L. Zavaleta, B.R. Smith, I. Walton, W. Doering, G. Davis, B. Shojaei, M.J. Natan, S.S. Gambhir, Multiplexed imaging of surface enhanced Raman scattering nanotags in living mice using noninvasive Raman spectroscopy, *Proc. Natl. Acad. Sci. U. S. A.* **106** (2009), 13511-13516.

[58] A.P.F. Turner, B.N. Chen, S.A. Piletsky, In vitro diagnostics in diabetes: Meeting the challenge, *Clin. Chem.* **45** (1999), 1596-1601.

[59] G.S. Wilson, Y.B. Hu, Enzyme based biosensors for in vivo measurements, *Chem. Rev.* **100** (2000), 2693-2704.

[60] R.J. Russell, M.V. Pishko, C.C. Gefrides, M.J. McShane, G.L. Cote, A fluorescence-based glucose biosensor using concanavalin A and dextran encapsulated in a poly(ethylene glycol) hydrogel, *Anal. Chem.* **71** (1999), 3126-3132.

[61] J.H. Pei, F. Tian, T. Thundat, Glucose biosensor based on the microcantilever, *Anal. Chem.* **76** (2004), 292-297.

[62] D.A. Stuart, C.R. Yonzon, X. Zhang, O. Lyandres, N.C. Shah, M.R. Glucksberg, J.T. Walsh, R.P. Van Duyne, Glucose Sensing Using Near-Infrared Surface-Enhanced Raman Spectroscopy: Gold Surfaces, 10-Day Stability, and Improved Accuracy, *Anal. Chem.* **77** (2005), 4013-4019.

[63] O. Lyandres, N.C. Shah, C.R. Yonzon, J.T. Walsh, M.R. Glucksberg, R.P. Van Duyne, Real-time glucose sensing by surface-enhanced Raman spectroscopy in bovine plasma facilitated by a mixed decanethiol/mercaptohexanol partition layer, *Anal. Chem.* **77** (2005), 6134-6139.

[64] D.B. Gomis, D.M. Tamayo, J.M. Alonso, Determination of monosaccharides in cider by reversed-phase liquid chromatography, *Anal. Chim. Acta.* **436** (2001), 173-180.

[65] M.L. Di Gioia, A. Leggio, A. Le Pera, A. Liguori, A. Napoli, C. Siciliano, G. Sindona, Quantitative analysis of human salivary glucose by gas chromatography-mass spectrometry, *J. Chromatogr., B: Anal. Technol. Biomed. Life Sci.* **801** (2004), 355-358.

[66] B.D. Cameron, H. Gorde, G.L. Cote, Development of an optical polarimeter for in vivo glucose monitoring, *Proc. SPIE* **3599** (1999), 43-49.

[67] D.C. Klonoff, Noninvasive blood glucose monitoring, *Diabetes Care* **20** (1997), 433-437.

[68] I. Gabriely, H. Shamoon, Transcutaneous glucose measurement using near-infrared spectroscopy during hypoglycemia, *Diabetes Care* **23** (2000), 1209-1210.

[69] L.A. Marquardt, M.A. Arnold, G.W. Small, Near-Infrared Spectroscopic Measurement of Glucose in a Protein Matrix, *Anal. Chem.* **65** (1993), 3271-3278.

[70] A.J. Berger, T.W. Koo, I. Itzkan, G. Horowitz, M.S. Feld, Multicomponent blood analysis by near-infrared Raman spectroscopy, *Appl. Opt.* **38** (1999), 2916-2926.

[71] A.M.K. Enejder, T.W. Koo, J. Oh, M. Hunter, S. Sasic, M.S. Feld, G.L. Horowitz, Blood analysis by Raman spectroscopy, *Opt. Lett.* **27** (2002), 2004-2006.

[72] O. Lyandres, J.M. Yuen, N.C. Shah, R.P. VanDuyne, J.T. Walsh, M.R. Glucksberg, Progress toward an in vivo surface-enhanced Raman spectroscopy glucose sensor, *Diabetes Technol. Ther.* **10** (2008), 257-265.

[73] K.E. Shafer-Peltier, C.L. Haynes, M.R. Glucksberg, R.P. Van Duyne, Toward a glucose biosensor based on surface-enhanced Raman scattering, *J. Am. Chem. Soc.* **125** (2003), 588-593.

[74] C.R. Yonzon, C.L. Haynes, X. Zhang, J.T. Walsh, R.P. Van Duyne, A Glucose Biosensor Based on Surface-Enhanced Raman Scattering: Improved Partition Layer, Temporal Stability, Reversibility, and Resistance to Serum Protein Interference, *Anal. Chem.* **76** (2003), 78-85.

[75] D.A. Stuart, J.M. Yuen, N.S.O. Lyandres, C.R. Yonzon, M.R. Glucksberg, J.T. Walsh, R.P. Van Duyne, In vivo glucose measurement by surface-enhanced Raman spectroscopy, *Anal. Chem.* **78** (2006), 7211-7215.

[76] A. Loren, J. Engelbrektsson, C. Eliasson, M. Josefson, J. Abrahamsson, K. Abrahamsson, Self-assembled monolayer coating for normalization of surface enhanced Raman spectra, *Nano Lett.* **4** (2004), 309-312.

[77] Z. Xiaoyu, N.C. Shah, R.P. Van Duyne, Sensitive and selective chem/bio sensing based on surface-enhanced Raman spectroscopy (SERS), *Vib. Spectrosc.* **42** (2006), 2-88.

[78] J.A. Dieringer, A.D. McFarland, N.C. Shah, D.A. Stuart, A.V. Whitney, C.R. Yonzon, M.A. Young, X.Y. Zhang, R.P. Van Duyne, Surface enhanced Raman spectroscopy: new materials, concepts, characterization tools, and applications, *Faraday Discuss.* **132** (2006), 9-26.

[79] P. Matousek, I.P. Clark, E.R.C. Draper, M.D. Morris, A.E. Goodship, N. Everall, M. Towrie, W.F. Finney, A.W. Parker, Subsurface probing in diffusely scattering media using spatially offset Raman spectroscopy, *Appl. Spectrosc.* **59** (2005), 393-400.

[80] J.M. Yuen, N.C. Shah, J.T. Walsh, Jr., M.R. Glucksberg, R.P. Van Duyne, Transcutaneous Glucose Sensing by Surface-Enhanced Spatially Offset Raman Spectroscopy in a Rat Model, *Anal. Chem.* **82** (2010), 8382-8385.

[81] K. Ma, J.M. Yuen, N.C. Shah, J.T. Walsh, M.R. Glucksberg, R.P. Van Duyne, In Vivo, Transcutaneous Glucose Sensing Using Surface-Enhanced Spatially Offset Raman Spectroscopy: Multiple Rats, Improved Hypoglycemic Accuracy, Low Incident Power, and Continuous Monitoring for Greater than 17 Days, *Anal. Chem.* **83** (2011), 9146-9152.

[82] Q. Tu, C. Chang, Diagnostic applications of Raman spectroscopy, *Nanomed.-Nanotechnol. Biol. Med.* **8** (2012), 545-558.

[83] Y. Oshima, H. Shinzawa, T. Takenaka, C. Furihata, H. Sato, Discrimination analysis of human lung cancer cells associated with histological type and malignancy using Raman spectroscopy, *J. Biomed. Opt.* **15** (2010), 017009.

[84] P. Crow, B. Barrass, C. Kendall, M. Hart-Prieto, M. Wright, R. Persad, N. Stone, The use of Raman spectroscopy to differentiate between different prostatic adenocarcinoma cell lines, *Brit. J. Cancer* **92** (2005), 2166-2170.

[85] A.S. Haka, Z. Volynskaya, J.A. Gardecki, J. Nazemi, R. Shenk, N. Wang, R.R. Dasari, M. Fitzmaurice, M.S. Feld, Diagnosing breast cancer using Raman spectroscopy: prospective analysis, *J. Biomed. Opt.* **14** (2009), 054023.

[86] B.W.D. de Jong, T.C. Bakker, K. Maquelin, T. van der Kwast, C.H. Bangma, D.J. Kok, G.J. Puppels, Discrimination between nontumor bladder tissue and tumor by Raman spectroscopy, *Anal. Chem.* **78** (2006), 7761-7769.

[87] A. Campion, P. Kambhampati, Surface-enhanced Raman scattering, *Chem. Soc. Rev.* **27** (1998), 241-250.

[88] J. Kneipp, H. Kneipp, K. Kneipp, SERS - a single-molecule and nanoscale tool for bioanalytics, *Chem. Soc. Rev.* **37** (2008), 1052-1060.

[89] P.C. Ray, S.A. Khan, A.K. Singh, D. Senapati, Z. Fan, Nanomaterials for targeted detection and photothermal killing of bacteria, *Chem. Soc. Rev.* **41** (2012), 3193-3209.

[90] M.B. Wabuyele, F. Yan, T. Vo-Dinh, Plasmonics nanoprobes: detection of single-nucleotide polymorphisms in the breast cancer BRCA1 gene, *Anal. Bioanal. Chem.* **398** (2010), 729-736.

[91] G.F. Wang, R.J. Lipert, M. Jain, S. Kaur, S. Chakraboty, M.P. Torres, S.K. Batra, R.E. Brand, M.D. Porter, Detection of the Potential Pancreatic Cancer Marker MUC4 in Serum Using Surface-Enhanced Raman Scattering, *Anal. Chem.* **83** (2011), 2554-2561.

[92] B. Yan, B.M. Reinhard, Identification of Tumor Cells through Spectroscopic Profiling of the Cellular Surface Chemistry, *J. Phys. Chem. Lett.* **1** (2010), 1595-1598.

[93] J. Yang, Z.Y. Wang, S.F. Zong, C.Y. Song, R.H. Zhang, Y.P. Cui, Distinguishing breast cancer cells using surface-enhanced Raman scattering, *Anal. Bioanal. Chem.* **402** (2012), 1093-1100.

[94] M. Lee, K. Lee, K.H. Kim, K.W. Oh, J. Choo, SERS-based immunoassay using a gold array-embedded gradient microfluidic chip, *Lab Chip* **12** (2012), 3720-3727.

[95] L.R. Allain, T. Vo-Dinh, Surface-enhanced Raman scattering detection of the breast cancer susceptibility gene BRCA1 using a silver-coated microarray platform, *Anal. Chim. Acta.* **469** (2002), 149-154.

[96] T. Vo-Dinh, L.R. Allain, D.L. Stokes, Cancer gene detection using surface-enhanced Raman scattering (SERS), *J. Raman Spectrosc.* **33** (2002), 511-516.

[97] X.Z. Li, T.Y. Yang, J.X. Lin, Spectral analysis of human saliva for detection of lung cancer using surface-enhanced Raman spectroscopy, *J. Biomed. Opt.* **17** (2012), 037003.

[98] J.C.Y. Kah, K.W. Kho, C.G.L. Lee, C.J.R. Sheppard, Z.X. Shen, K.C. Soo, M.C. Olivo, Early diagnosis of oral cancer based on the surface plasmon resonance of gold nanoparticles, *Int. J. Nanomed.* **2** (2007), 785-798.

[99] D. Lin, S.Y. Feng, J.J. Pan, Y.P. Chen, J.Q. Lin, G.N. Chen, S.S. Xie, H.S. Zeng, R. Chen, Colorectal cancer detection by gold nanoparticle based surface-enhanced Raman spectroscopy of blood serum and statistical analysis, *Opt. Express* **19** (2011), 13565-13577.

[100]S.Y. Feng, R. Chen, J.Q. Lin, J.J. Pan, Y.A. Wu, Y.Z. Li, J.S. Chen, H.S. Zeng, Gastric cancer detection based on blood plasma surface-enhanced Raman spectroscopy excited by polarized laser light, *Biosens. Bioelectron.* **26** (2011), 3167-3174.

[101]Y. Zhang, H. Hong, W.B. Cai, Imaging with Raman Spectroscopy, *Curr. Pharm. Biotechnol.* **11** (2010), 654-661.

[102]M.C. Breitkreitz, R.J. Poppi, Trends in Raman chemical imaging, *Biomedical Spectroscopy and Imaging* **1** (2012), 159-183.

[103]Y. Zhang, H. Hong, D.V. Myklejord, W.B. Cai, Molecular Imaging with SERS-Active Nanoparticles, *Small* **7** (2011), 3261-3269.

[104]M.V. Yigit, Z. Medarova, In-vivo and ex-vivo applications of gold nanoparticles for biomedical SERS imaging, *Am. J. Nucl. Med. Mol. Imaging* **2** (2012), 232–241.

[105]C.L. Zavaleta, M.F. Kircher, S.S. Gambhir, Raman's "Effect" on Molecular Imaging, *J. Nucl. Med.* **52** (2011), 1839-1844.

[106]R.G. Blasberg, Imaging update: New windows, new views, *Clin. Cancer Res.* **13** (2007), 3444-3448.

[107]S. Kaur, G. Venktaraman, M. Jain, S. Senapati, P.K. Garg, S.K. Batra, Recent trends in antibody-based oncologic imaging, *Cancer Lett.* **315** (2012), 97-111.

[108]G. von Maltzahn, A. Centrone, J.H. Park, R. Ramanathan, M.J. Sailor, T.A. Hatton, S.N. Bhatia, SERS-Coded Gold Nanorods as a Multifunctional Platform for Densely Multiplexed Near-infrared Imaging and Photothermal Heating, *Adv. Mater.* **21** (2009), 3175-3180.

[109]Y. Cui, X.-S. Zheng, B. Ren, R. Wang, J. Zhang, N.-S. Xia, Z.-Q. Tian, Au@organosilica multifunctional nanoparticles for the multimodal imaging, *Chem. Sci.* **2** (2011), 1463-1469.

[110]L. Jiang, J. Qian, F. Cai, S. He, Raman reporter-coated gold nanorods and their applications in multimodal optical imaging of cancer cells, *Anal. Bioanal. Chem.* **400** (2011), 2793-2800.

[111]Y. Wang, L. Chen, P. Liu, Biocompatible Triplex Ag@SiO2@mTiO2 Core–Shell Nanoparticles for Simultaneous Fluorescence-SERS Bimodal Imaging and Drug Delivery, *Chemistry* **18** (2012), 5935-5943.

[112]M.V. Yigit, L. Zhu, M.A. Ifediba, Y. Zhang, K. Carr, A. Moore, Z. Medarova, Noninvasive MRI-SERS Imaging in Living Mice Using an Innately Bimodal Nanomaterial, *ACS Nano* **5** (2011), 1056-1066.

[113]J.P. Camden, J.A. Dieringer, J. Zhao, R.P. Van Duyne, Controlled Plasmonic Nanostructures for Surface-Enhanced Spectroscopy and Sensing, *Acc. Chem. Res.* **41** (2008), 1653-1661.

[114]R. Gordon, D. Sinton, K.L. Kavanagh, A.G. Brolo, A new generation of sensors based on extraordinary optical transmission, *Acc. Chem. Res.* **41** (2008), 1049-1057.

[115]K.L. Kelly, E. Coronado, L.L. Zhao, G.C. Schatz, The Optical Properties of Metal Nanoparticles: The Influence of Size, Shape, and Dielectric Environment, *J. Phys. Chem. B* **107** (2002), 668-677.

[116]J.B. Jackson, N.J. Halas, Surface-enhanced Raman scattering on tunable plasmonic nanoparticle substrates, *Proc. Natl. Acad. Sci. U. S. A.* **101** (2004), 17930-17935.

[117]E.C. Le Ru, E. Blackie, M. Meyer, P.G. Etchegoin, Surface Enhanced Raman Scattering Enhancement Factors: A Comprehensive Study, *J. Phys. Chem. C* **111** (2007), 13794-13803.

[118]G. Frens, Particle size and sol stability in metal colloids, *Kolloid Z. Z. Polym.* **250** (1972), 736-741.

[119]B.V. Enustun, J. Turkevich, Coagulation of Colloidal Gold, *J. Am. Chem. Soc.* **85** (1963), 3317-3328.

[120]M. Grosserueschkamp, C. Nowak, D. Schach, W. Schaertl, W. Knoll, R.L.C. Naumann, Silver Surfaces with Optimized Surface Enhancement by Self-Assembly of Silver Nanoparticles for Spectroelectrochemical Applications, *J. Phys. Chem. C* **113** (2009), 17698-17704.

[121]L. Jiang, Y. Sun, C. Nowak, A. Kibrom, C. Zou, J. Ma, H. Fuchs, S. Li, L. Chi, X. Chen, Patterning of Plasmonic Nanoparticles into Multiplexed One-Dimensional Arrays Based on Spatially Modulated Electrostatic Potential, *ACS Nano* **5** (2011), 8288-8294.

[122]Y. Xiong, Y. Xia, Shape-Controlled Synthesis of Metal Nanostructures: The Case of Palladium, *Adv. Mater.* **19** (2007), 3385-3391.

[123]P.M. Ajayan, L.D. Marks, Quasimelting and phases of small particles, *Phys. Rev. Lett.* **60** (1988), 585-587.

[124]Y. Xiong, J.M. McLellan, J. Chen, Y. Yin, Z.-Y. Li, Y. Xia, Kinetically Controlled Synthesis of Triangular and Hexagonal Nanoplates of Palladium and Their SPR/SERS Properties, *J. Am. Chem. Soc.* **127** (2005), 17118-17127.

[125]Y. Xiong, H. Cai, B.J. Wiley, J. Wang, M.J. Kim, Y. Xia, Synthesis and Mechanistic Study of Palladium Nanobars and Nanorods, *J. Am. Chem. Soc.* **129** (2007), 3665-3675.

[126]R.G. Freeman, K.C. Grabar, K.J. Allison, R.M. Bright, J.A. Davis, A.P. Guthrie, M.B. Hommer, M.A. Jackson, P.C. Smith, D.G. Walter, M.J. Natan, Self-Assembled Metal Colloid Monolayers: An Approach to SERS Substrates, *Science* **267** (1995), 1629-1632.

[127]T. Felicia, B. Monica, B. Lucian, A. Simion, Controlling gold nanoparticle assemblies for efficient surface-enhanced Raman scattering and localized surface plasmon resonance sensors, *Nanotechnology* **18** (2007), 255702.

[128]M. Muniz-Miranda, B. Pergolese, A. Bigotto, A. Giusti, Stable and efficient silver substrates for SERS spectroscopy, *J. Colloid Interface Sci.* **314** (2007), 540-544.

[129]S.J. Lee, J.M. Baik, M. Moskovits, Polarization-Dependent Surface-Enhanced Raman Scattering from a Silver-Nanoparticle-Decorated Single Silver Nanowire, *Nano Lett.* **8** (2008), 3244-3247.

[130]C.J. Addison, S.O. Konorov, A.G. Brolo, M.W. Blades, R.F.B. Turner, Tuning Gold Nanoparticle Self-Assembly for Optimum Coherent Anti-Stokes Raman Scattering and Second Harmonic Generation Response, *J. Phys. Chem. C* **113** (2009), 3586-3592.

[131]C.J. Addison, A.G. Brolo, Nanoparticle-Containing Structures as a Substrate for Surface-Enhanced Raman Scattering, *Langmuir* **22** (2006), 8696-8702.

[132]C. Caro, C. López-Cartes, P. Zaderenko, J.A. Mejías, Thiol-immobilized silver nanoparticle aggregate films for surface enhanced Raman scattering, *J. Raman Spectrosc.* **39** (2008), 1162-1169.

[133]R. Gunawidjaja, E. Kharlampieva, I. Choi, V.V. Tsukruk, Bimetallic Nanostructures as Active Raman Markers: Gold-Nanoparticle Assembly on 1D and 2D Silver Nanostructure Surfaces, *Small* **5** (2009), 2460-2466.

[134]W. Yuan, C.M. Li, Direct Modulation of Localized Surface Plasmon Coupling of Au Nanoparticles on Solid Substrates via Weak Polyelectrolyte-Mediated Layer-by-Layer Self Assembly, *Langmuir* **25** (2009), 7578-7585.

[135]R.F. Aroca, P.J.G. Goulet, D.S. dos Santos, R.A. Alvarez-Puebla, O.N. Oliveira, Silver Nanowire Layer-by-Layer Films as Substrates for Surface-Enhanced Raman Scattering, *Anal. Chem.* **77** (2004), 378-382.

[136]J. Zeng, H. Jia, J. An, X. Han, W. Xu, B. Zhao, Y. Ozaki, Preparation and SERS study of triangular silver nanoparticle self-assembled films, *J. Raman Spectrosc.* **39** (2008), 1673-1678.

[137]H.-W. Cheng, W.-Q. Luo, G.-L. Wen, S.-Y. Huan, G.-L. Shen, R.-Q. Yu, Surface-enhanced Raman scattering based detection of bacterial biomarker and potential surface reaction species, *Analyst* **135** (2010), 2993-3001.

[138]V. Yuli, B. Antony, V. Olga, J. Wenlong, L. Quinn, Demagnification in proximity x-ray lithography and extensibility to 25 nm by optimizing Fresnel diffraction, *J. Phys. D: Appl. Phys.* **32** (1999), L114.

[139]J.C. Wolfe, B.P. Craver, Neutral particle lithography: a simple solution to charge-related artefacts in ion beam proximity printing, *J. Phys. D: Appl. Phys.* **41** (2008), 024007.

[140]B.A. Wacaser, M.J. Maughan, I.A. Mowat, T.L. Niederhauser, M.R. Linford, R.C. Davis, Chemomechanical surface patterning and functionalization of silicon surfaces using an atomic force microscope, *Appl. Phys. Lett.* **82** (2003), 808-810.

[141]M. Kahl, E. Voges, S. Kostrewa, C. Viets, W. Hill, Periodically structured metallic substrates for SERS, *Sens. Actuators, B* **51** (1998), 285-291.

[142]Q. Yu, P. Guan, D. Qin, G. Golden, P.M. Wallace, Inverted Size-Dependence of Surface-Enhanced Raman Scattering on Gold Nanohole and Nanodisk Arrays, *Nano Letters* **8** (2008), 1923-1928.

[143]Y.J. Liu, Z.Y. Zhang, Q. Zhao, Y.P. Zhao, Revisiting the separation dependent surface enhanced Raman scattering, *Appl. Phys. Lett.* **93** (2008), 173106-3.

[144]L. Gunnarsson, E.J. Bjerneld, H. Xu, S. Petronis, B. Kasemo, M. Kall, Interparticle coupling effects in nanofabricated substrates for surface-enhanced Raman scattering, *Appl. Phys. Lett.* **78** (2001), 802-804.

[145]P. Frank, J. Srajer, A. Schwaighofer, A. Kibrom, C. Nowak, Double-layered nanoparticle stacks for spectro-electrochemical applications, *Opt. Lett.* **37** (2012), 3603-3605.

[146]N. Felidj, S.L. Truong, J. Aubard, G. Levi, J.R. Krenn, A. Hohenau, A. Leitner, F.R. Aussenegg, Gold particle interaction in regular arrays probed by surface enhanced Raman scattering, *J. Chem. Phys.* **120** (2004), 7141-7146.

[147]Y.Z. Chu, K.B. Crozier, Experimental study of the interaction between localized and propagating surface plasmons, *Opt. Lett.* **34** (2009), 244-246.

[148]Y. Chu, M.G. Banaee, K.B. Crozier, Double-Resonance Plasmon Substrates for Surface-Enhanced Raman Scattering with Enhancement at Excitation and Stokes Frequencies, *ACS Nano* **4** (2010), 2804-2810.

[149]C.L. Haynes, R.P. Van Duyne, Nanosphere Lithography: A Versatile Nanofabrication Tool for Studies of Size-Dependent Nanoparticle Optics, *J. Phys. Chem. B* **105** (2001), 5599-5611.

[150]T.R. Jensen, M.D. Malinsky, C.L. Haynes, R.P. Van Duyne, Nanosphere Lithography: Tunable Localized Surface Plasmon Resonance Spectra of Silver Nanoparticles, *J. Phys. Chem. B* **104** (2000), 10549-10556.

[151]J.C. Hulteen, D.A. Treichel, M.T. Smith, M.L. Duval, T.R. Jensen, R.P. Van Duyne, Nanosphere Lithography: Size-Tunable Silver Nanoparticle and Surface Cluster Arrays, *J. Phys. Chem. B* **103** (1999), 3854-3863.

[152]C.L. Haynes, R.P. Van Duyne, Plasmon-Sampled Surface-Enhanced Raman Excitation Spectroscopy†, *J. Phys. Chem. B* **107** (2003), 7426-7433.

[153]L.Y. Wu, B.M. Ross, L.P. Lee, Optical Properties of the Crescent-Shaped Nanohole Antenna, *Nano Letters* **9** (2009), 1956-1961.

[154]R. Bukasov, J.S. Shumaker-Parry, Highly Tunable Infrared Extinction Properties of Gold Nanocrescents, *Nano Letters* **7** (2007), 1113-1118.

[155]R. Bukasov, T.A. Ali, P. Nordlander, J.S. Shumaker-Parry, Probing the Plasmonic Near-Field of Gold Nanocrescent Antennas, *ACS Nano* **4** (2010), 6639-6650.

[156]W. Knoll, Interfaces and thin films as seen by bound electromagnetic waves, *Annu. Rev. Phys. Chem.* **49** (1998), 569-638.

[157]S.A. Maier, *Plasmonics: Fundamentals and Applications*. Springer, New York, 2007.

[158]J. Zhao, A.O. Pinchuk, J.M. McMahon, S. Li, L.K. Ausman, A.L. Atkinson, G.C. Schatz, Methods for Describing the Electromagnetic Properties of Silver and Gold Nanoparticles, *Acc. Chem. Res.* **41** (2008), 1710-1720.

[159]G. Mie, Beiträge zur Optik trüber Medien, speziell kolloidaler Metallösungen, *Ann. Phys.* **330** (1908), 377-445.

[160]R. Gans, Über die Form ultramikroskopischer Goldteilchen, *Ann. Phys.* **342** (1912), 881-900.

[161]I. Abdulhalim, M. Zourob, A. Lakhtakia, Surface Plasmon Resonance for Biosensing: A Mini-Review, *Electromagnetics* **28** (2008), 214-242.

[162]G. Shvets, Y.A. Urzhumov, Electric and magnetic properties of sub-wavelength plasmonic crystals, *J. Opt. A: Pure Appl. Opt.* **7** (2005), S23-S31.

[163]K. Yee, Numerical solution of initial boundary value problems involving maxwell's equations in isotropic media, *IEEE Trans. Antennas Propag.* **14** (1966), 302-307.

[164]A. Taflove, M.E. Brodwin, Numerical Solution of Steady-State Electromagnetic Scattering Problems Using the Time-Dependent Maxwell's Equations, *IEEE Trans. Microw. Theory Techn.* **23** (1975), 623-630.

[165]A. Taflove, Application of the Finite-Difference Time-Domain Method to Sinusoidal Steady-State Electromagnetic-Penetration Problems, *IEEE Trans. Electromagn. Compat.* **EMC-22** (1980), 191-202.

[166]D.S. Katz, E.T. Thiele, A. Taflove, Validation and extension to three dimensions of the Berenger PML absorbing boundary condition for FD-TD meshes, *IEEE Microw. Guided Wave Lett.* **4** (1994), 268-270.

[167]J.-P. Berenger, A perfectly matched layer for the absorption of electromagnetic waves, *J. Comput. Phys.* **114** (1994), 185-200.

[168]S.D. Gedney, An anisotropic perfectly matched layer-absorbing medium for the truncation of FDTD lattices, *IEEE Trans. Antennas Propag.* **44** (1996), 1630-1639.

[169]J.A. Roden, S.D. Gedney, Convolution PML (CPML): An efficient FDTD implementation of the CFS–PML for arbitrary media, *Microw. Opt. Techn. Let.* **27** (2000), 334-339.

[170]H. De Raedt, K. Michielsen, J.S. Kole, M.T. Figge, Solving the Maxwell equations by the Chebyshev method: a one-step finite-difference time-domain algorithm, *IEEE Trans. Antennas Propag.* **51** (2003), 3155-3160.

[171]I. Ahmed, C. Eng-Kee, L. Er-Ping, C. Zhizhang, Development of the Three-Dimensional Unconditionally Stable LOD-FDTD Method, *IEEE Trans. Antennas Propag.* **56** (2008), 3596-3600.

[172]E.M.a.P. Purcell, C.R., Scattering and Absorption of Light by Nonspherical Dielectric Grains, *Astrophys. J.* **186** (1973), 705-714.

[173]M.A. Yurkin, A.G. Hoekstra, The discrete dipole approximation: An overview and recent developments, *J. Quant. Spectrosc. Radiat. Transfer* **106** (2007), 558-589.

[174]B.T. Draine, P.J. Flatau, Discrete-dipole approximation for periodic targets: theory and tests, *J. Opt. Soc. Am. A* **25** (2008), 2693-2703.

[175]J.M. Donald, A. Golden, S.G. Jennings, Opendda: a Novel High-Performance Computational Framework for the Discrete Dipole Approximation, *Int. J. High. Perform. C.* **23** (2009), 42-61.

[176]M.D. McMahon. Effects of Geometrical Order on the Linear and Nonlinear Optical Properties of Metal Nanoparticles. Dissertation, Vanderbilt University, Nashville, Tennessee, 2006.

[177]B.S. Guiton, V. Iberi, S. Li, D.N. Leonard, C.M. Parish, P.G. Kotula, M. Varela, G.C. Schatz, S.J. Pennycook, J.P. Camden, Correlated Optical Measurements and Plasmon Mapping of Silver Nanorods, *Nano Lett.* **11** (2011), 3482-3488.

[178]R. Courant, Variational methods for the solution of problems of equilibrium and vibrations, *Bull. Amer. Math. Soc.* **49** (1943), 1-23.

[179]K. Ho-Le, Finite element mesh generation methods: a review and classification, *Comput. Aided Des.* **20** (1988), 27-38.

[180]R. Coccioli, T. Itoh, G. Pelosi, P.P. Silvester, Finite-element methods in microwaves: a selected bibliography, *IEEE Antennas Propag. Mag.* **38** (1996), 34-48.